SGD-SM 2.0: An Improved Seamless Global Daily Soil Moisture Long-term Dataset From 2002 to 2022

Qiang Zhang[1], Qiangqiang Yuan[2 *], Taoyong Jin[2 *], Meiping Song[3], and Fujun Sun[4]

[1]State Key Laboratory of Information Engineering, Survey Mapping and Remote Sensing, Wuhan University, China
[2]School of Geodesy and Geomatics, Wuhan University, China
[3]CHIRS, Information Science and Technology College, Dalian Maritime University, China
[4]CASIC Research Institute of Intelligent Decision Engineering, Beijing, China

Correspondence: Qiangqiang Yuan (yqiang86@gmail.com) and Taoyong Jin (tyjin@sgg.whu.edu.cn)

Abstract. Satellite-based daily soil moisture products inevitably exist the drawbacks of low-coverage rate in global land, because of the satellite orbit covering scopes and the limitations of soil moisture retrieving models. To solve this issue, Zhang et al. (2021) generated seamless global daily soil moisture (SGD-SM 1.0) products for the years 2013~2019. Nevertheless, there are still several shortages in SGD-SM 1.0 products, especially on temporal range, sudden extreme weather condition, and sequential time-series information. In this work, we develop an improved seamless global daily soil moisture (SGD-SM 2.0) dataset from 2002 to 2022, to overcome above shortages. SGD-SM 2.0 uses three sensors AMSR-E, AMSR2 and WindSat. Global daily precipitation products are assimilated into the proposed reconstructing model. We propose an integrated long short-term memory convolutional neural network (LSTM-CNN) to fill the gaps and missing regions in daily soil moisture products. In-situ validation and time-series validation testify the reconstructing accuracy and availability of SGD-SM 2.0 (R: 0.672, RMSE: 0.096, MAE: 0.078). The time-series curves of the improved SGD-SM 2.0 are consistency with the original daily time-series soil moisture and precipitation distribution. Compared with SGD-SM 1.0, the improved SGD-SM 2.0 outperforms on reconstructing accuracy and time-series consistency. SGD-SM 2.0 products are recorded at **https://doi.org/10.5281/zenodo.6041561** (Zhang et al., 2022).

1 Introduction

Surface soil moisture acts as a significant part on global hydrology and meteorology, especially for forecasting drought and flood disasters (Wigneron et al., 1999; Long et al., 2014; Brocca et al., 2018). In recent years, satellite-based soil moisture retrieving data has been rapidly progressed on both global and daily monitoring (Shi et al., 2006; Dorigo et al., 2012; Al Bitar et al., 2017). For example, AMSR-E, AMSR2, WindSat global daily soil moisture products and so on (Fan et al., 2004). These quantitative products have been widely utilized for global and long-term hydrological analysis and forecast (Chen et al., 2021).

However, because of the limitations of soil moisture retrieving models and satellite orbital covering scopes, the obtained daily soil moisture products are fragmentary and incomplete (Shi et al., 2002; Enenkel et al, 2016; Meng et al., 2021). These global daily soil moisture products exist plenty of gaps or missing regions, as shown in Fig. 1(a) and (b). Actually, the land coverage rate is only about 20%~80% in daily AMSR-E/2 and WindSat quantitative products (Long et al., 2019).

Earth System
Science
Data

(a) Original SM in 2019.6.1   (b) Reconstructing SM in 2019.6.1
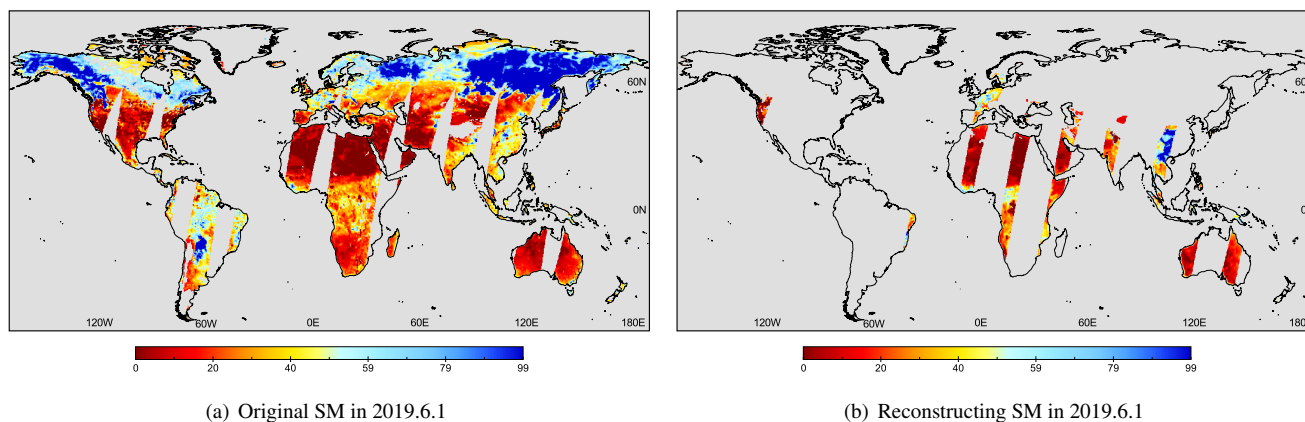
Figure 1. Daily soil moisture products of AMSR-E and WindSat

To settle this adverse effect for global soil moisture applications, most of works adopted the temporal averaging operation
such as monthly, quarterly, or yearly averaging (Schaffitel et al., 2020; Guevara et al., 2021; Wang et al., 2021). This strategy
could usually acquire full-coverage soil moisture products via averaging abundant daily products. Nevertheless, temporal aver-
aging operation is also a two-edged sword. Firstly, it directly replaces daily temporal resolution with low-frequency temporal
resolution (Rebel et al., 2012; Long et al., 2020), which greatly lowers the utilization of daily soil moisture products. Secondly,
temporal averaging operation disregards the specific spatial distribution of daily products, and neglects the sequential time-
series changing characteristic (Zeng et al., 2015; Wang et al., 2021). In other word, monthly, quarterly, or yearly averaging
strategy destroys the original characteristics for daily soil moisture products.

To address this issue, Zhang et al. (2021) generated a seamless, global, daily soil moisture (named SGD-SM 1.0) dataset from
2013 to 2019. The spatial resolution is denoted as $0.25°$ (about 25km). SGD-SM 1.0 relies on the deep spatio-temporal partial
convolutional model to fill the gaps or missing regions in daily soil moisture products. Then three validations are performed
to verify the reliability of SGD-SM 1.0 products. Relevant quantitative indexes and results demonstrate that SGD-SM 1.0
products can be extended for global, daily and full-coverage soil moisture measurements.

SGD-SM 1.0 maintains the original high-frequency daily temporal-resolution, and effectively enhances the utilization of
global daily soil moisture products. However, SGD-SM 1.0 also exists several weaknesses and limitations. Detailed descriptions
are listed as follows:

1) SGD-SM 1.0 only uses single sensor (AMSR2), and the temporal range is insufficient with just seven years. While global
soil moisture analysis and applications generally need longer-term and more multi-sensors products. The application range of
SGD-SM 1.0 is still limited.

2) SGD-SM 1.0 ignores the sporadic extreme weather condition for one day. If it occurs a sporadic precipitation, SGD-SM
1.0 usually behaves with poor performance under this condition. The main reason is that SGD-SM 1.0 relies on the internal
spatio-temporal correlation, which not considers the external environmental factors.

3) Although SGD-SM 1.0 employs 3-D partial convolutional neural network to exploit both spatial and temporal feature, it is still insufficient for utilizing sequential time-series information. For daily soil moisture products, how to effectively reconstruct gaps missing regions through interrelated temporal information is significant.

Based on SGD-SM 1.0 and above considerations, we develop an improved seamless global daily soil moisture (SGD-SM 2.0) dataset for the years 2002-2022 in this work. Compared with SGD-SM 1.0, the main improvements and contributions of SGD-SM 2.0 are listed as follows:

★ SGD-SM 2.0 uses three passive microwave sensors (AMSR-E, WindSat, and AMSR2). Temporal range of SGD-SM 2.0 is extended to twenty years from 2002 to 2022. Compared with SGD-SM 1.0, the application scope of SGD-SM 2.0 can be enlarged through these long-term soil moisture products.

★ SGD-SM 2.0 introduces the global daily precipitation products into the reconstructing framework. Through assimilating auxiliary precipitation information, SGD-SM 2.0 can consider the sudden extreme weather condition for single day in global daily soil moisture products.

★ SGD-SM 2.0 develops an integrated long short-term memory convolutional neural network (LSTM-CNN) to fill the gaps and missing regions in these daily products. The proposed LSTM-CNN model simultaneously utilizes recurrent time-series information and spatial information for generating SGD-SM 2.0 products.

★ In-situ validation and time-series validation testify the reconstructing accuracy and availability of SGD-SM 2.0 products (R: 0.672, RMSE: 0.096, MAE: 0.078). The time-series curves of the improved SGD-SM 2.0 products are also consistency with the original daily time-series soil moisture values.

The outline of this paper is arranged below. Sect.2 provides a description of products and data description used in this work. Sect. 3 gives the methodology of the proposed reconstructing framework for SGD-SM 2.0. Sect. 4 lists the experimental results of SGD-SM 2.0 products. Sect. 5 discusses the comparisons between SGD-SM 1.0 and SGD-SM 2.0, especially on reconstructing accuracy and time-series consistency. Finally, the conclusion and outlook are summarized in Sect. 6.

2 Products and data description

In this work, we simultaneously assimilate satellite-based soil moisture products and precipitation products to generate SGD-SM 2.0 dataset. The in-situ soil moisture sites are employed to validate the reconstructing precision of SGD-SM 2.0. Detailed descriptions are listed as follows.

2.1 Satellite-based soil moisture products

AMSR-E/2 and WindSat global daily soil moisture products are utilized from 2002 to 2022. These three sensors are on-boarded at Aqua satellite, GCOM-W1 and Coriolis satellite, respectively (Nepal et al., 2021). The spatial resolution is all 0.25° grid (about 25km) in these products, as depicted in Fig. 1(a)-(c). The retrieving model adopts the land parameter retrieval model

(LPRM) for AMSR-E, WindSat, and AMSR2 products (McColl et al., 2017). We select the descending orbit (night-time), and 6.9 GHz band for all these soil moisture products. These datasets are all recorded at GES DISC website.

The time-series range of AMSR-E sensor starts from 2002.06.19 and ends to 2011.10.04 (Njoku et al., 2003; Shi et al., 2008). The time-series range of WindSat sensor starts from 2003.02.01 and ends to 2012.08.02. The time-series range of
80   AMSR2 sensor starts from 2012.07.03 and continues to current date (Zeng et al., 2020). In consideration of the low-coverage rate in WindSat dataset, we just use WindSat global daily products from 2011.10.5 to 2012.07.02, for acquiring sequential daily products. These recorded AMSR-E and AMSR2 global daily products are all employed for generating SGD-SM 2.0 products. The daily coverage rate curves of these three global quantitative products are depicted in Fig. 2(a)-(c), respectively.

(a) Daily coverage rate curve of 2003   (b) Daily coverage rate curve of 2012   (c) Daily coverage rate curve of 2021
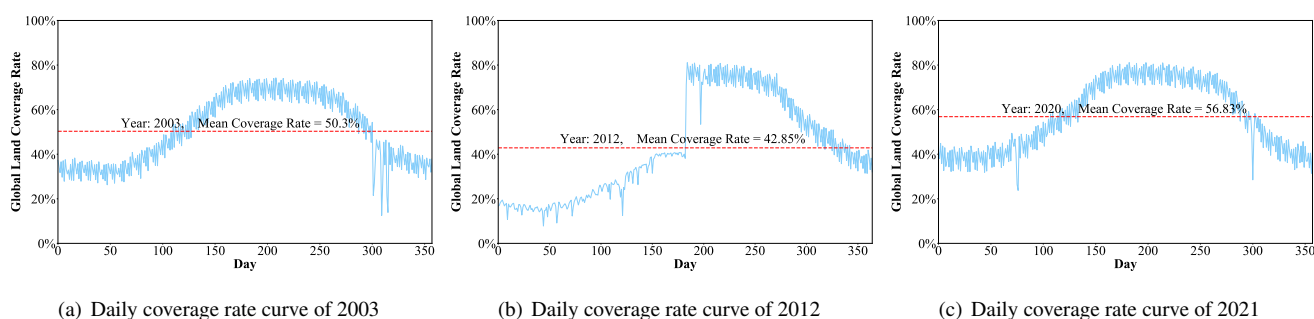
Figure 2. Daily coverage rate curves of AMSR-E, WindSat, and AMSR2 soil moisture products in 2002, 2012, and 2021.

2.2   Precipitation products

85   Precipitation usually exists the high correlation with surface soil moisture (Pellarin et al., 2009; Brocca et al., 2014; Sun and Fu, 2021). Therefore, we assimilate the precipitation products into the proposed SGD-SM 2.0 dataset to improve the reconstructing accuracy. The IMERG global daily precipitation V6 products are employed for the years 2002~2022 (Massari et al., 2020). These precipitation products are derived from multiple precipitation-relevant satellite passive microwave sensors, as portrayed in Fig. 3(a). The spatial resolution denotes as 0.1° grid (about 10km) in IMERG level 3 global daily final precipitation
90   products. To keep the uniformity with soil moisture products, the spatial downsampling operation is carried out for the original IMERG precipitation products from 0.1° to 0.25°. These precipitation products were all downloaded from GES DISC (Brocca et al., 2019; Berg et al., 2021; Škrk et al., 2021).

2.3   In-situ soil moisture data

In-situ soil moisture sites are significant for testifying the satellite-based products (Brocca et al., 2014). These sites provide
95   high-precision surface soil moisture values. Relied on in-situ data, the quantitative indexes could be derived for the proposed SGD-SM 2.0 dataset. ISMN unites global in-situ surface data, which has been widely applied for hydrology and soil moisture validation (Dorigo et al., 2011; Wigneron et al., 2013; Dorigo et al., 2013). We select 121 stations from ISMN from 2002 to 2022 and match them with corresponding soil moisture product in SGD-SM 2.0 (Zhang et al., 2020). The spatial distribution

of these selected in-situ data is displayed in Fig. 3(b). The in-situ validation results of SGD-SM 2.0 and the reconstructing

100 accuracy comparisons with SGD-SM 1.0 are given in section 4.2 and section 5.1, respectively.

(a) IMERG precipitation in 2019.06.05

(b) Spatial distribution of selected in-situ data
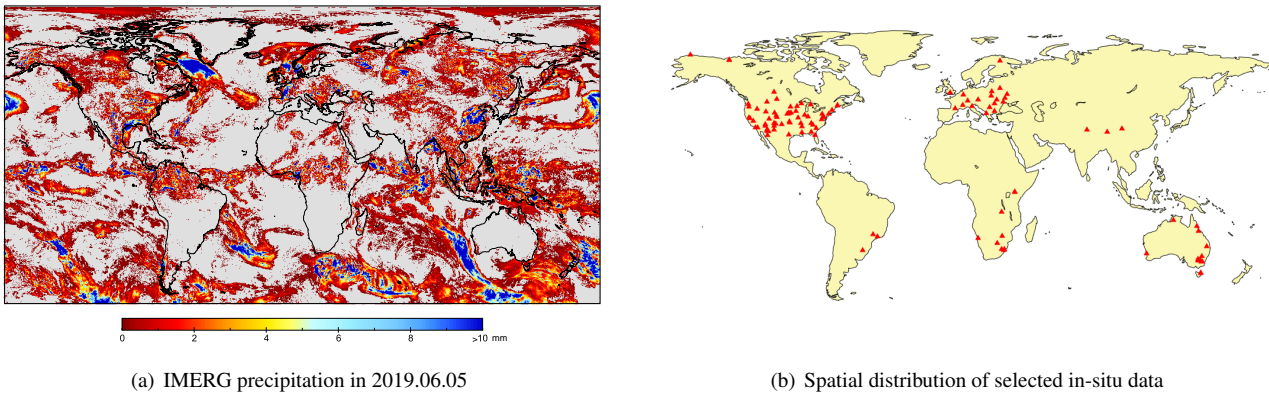
Figure 3. IMERG global daily precipitation and selected in-situ data.

3 Methodology

The schematic of the proposed work is depicted in Fig. 4. Different from SGD-SM 1.0, we simultaneously assimilate global daily precipitation products with global daily soil moisture products into SGD-SM 2.0. An integrated long short-term memory convolutional neural network (LSTM-CNN) reconstructing model is developed to fill the gap and missing regions in global

105 daily soil moisture products. Finally, we recursively generate the seamless daily soil moisture products in SGD-SM 2.0 dataset. Detailed descriptions of the proposed LSTM-CNN reconstructing model, training and optimization are stated below.

3.1 LSTM-CNN reconstructing model

As shown in Fig. 4, original global daily soil moisture product in date T and its corresponding global daily precipitation product in the same date are utilized as the input data of the proposed framework. Firstly, the precipitation data in date T is

110 transformed as the vector value P_T through a full-connected (FC in Fig. 4) layer. We employ the partial convolutional neural network (Partial CNN in Fig. 4) to extract the spatial feature of soil moisture product in date T. Different from the common CNN (Yuan et al., 2019), partial CNN can effectively acquire the spatial information within valid regions, and eliminate the invalid information within gap or soil moisture missing regions (Zhang et al., 2018). We applied partial CNN for generating SGD-SM 1.0 dataset. Due to its effectiveness on incomplete soil moisture products, the partial CNN is also used in this work

115 for generating SGD-SM 2.0 dataset. The formula of partial CNN in this work is determined as follow:

$$\mathbf{S}'_{(m,n)} = \begin{cases} \mathbf{W}^{\top}(\mathbf{S}_{(m,n)} \otimes \mathbf{M}_{(m,n)}) \frac{\left\|\mathbf{1}_{(m,n)}\right\|_1}{\left\|\mathbf{M}_{(m,n)}\right\|_1} + b, & \left\|\mathbf{M}_{(m,n)}\right\|_1 \neq 0 \\ 0, & otherwise \end{cases} \quad (1)$$
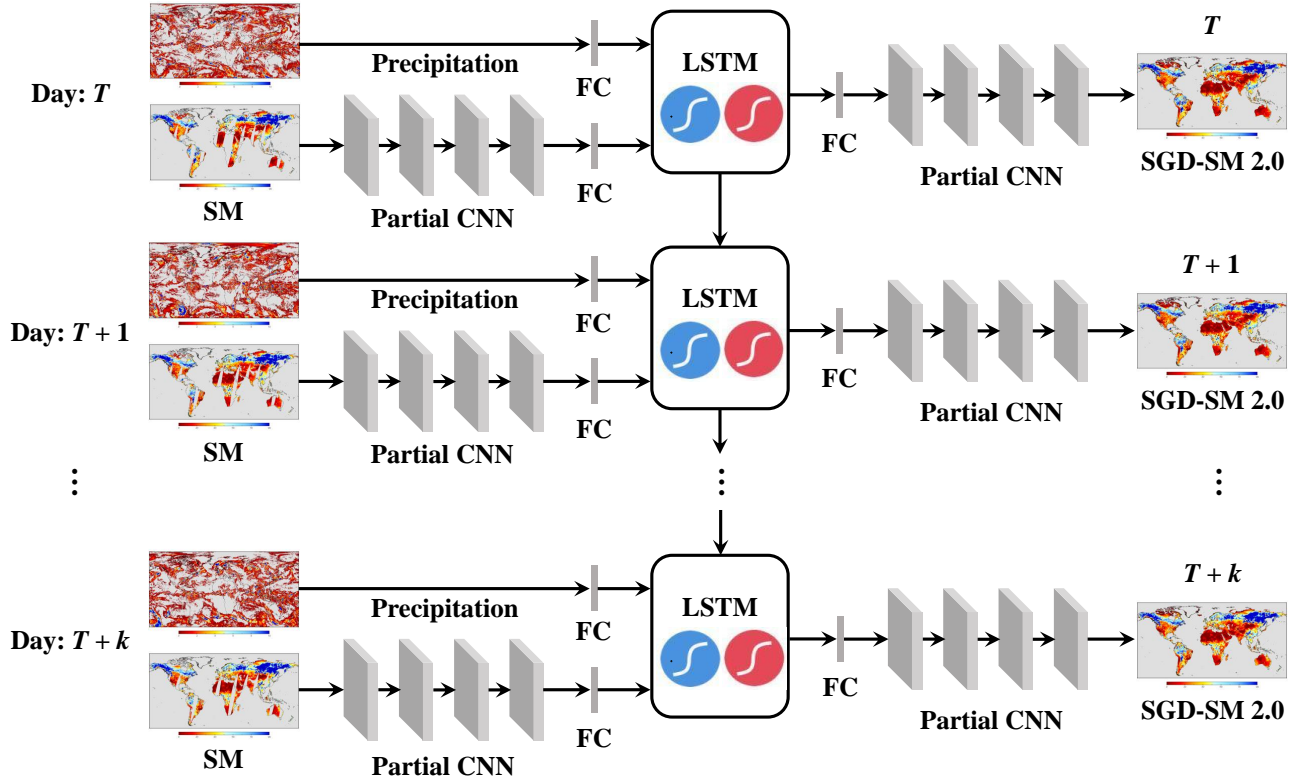
Figure 4. Schematic of the proposed framework to generate SGD-SM 2.0 products.

where $\mathbf{M}$ denotes the mask of its corresponding soil moisture product $\mathbf{S}$. 0 and 1 refer to the invalid and valid point in mask $\mathbf{M}$. $\mathbf{W}$ and b stand for trainable weighted and offset arguments in partial CNN, respectively. $\otimes$ represents the dot product operation, to exclude the invalid information in gap or missing regions through mask data. Subsequently, current mask $\mathbf{M}$
120 needs to regenerated under the below paradigm: On condition that the partial CNN can fill more than one valid element of the corresponding regions, we flag this point as valid information in the regenerated mask. The mask regenerated formula is defined as follow (Zhang et al., 2020):

$$\mathbf{M}'_{(m,n)} = \begin{cases} \mathbf{L}_{(m,n)}, & \left\|\mathbf{M}_{(m,n)}\right\|_1 \neq 0 \\ 0, & other \end{cases} \tag{2}$$

where $\mathbf{L}_{(m,n)}$ stand for Earth land in position (m, n). It should be noted that the Earth land mask includes 6 continents and
125 neglects all regions of Antarctica and most regions of Greenland. The main reason is that these omitted regions are perennially covered with snowy or frozen land (Zhao et al., 2021).

After four partial CNN layers in Fig. 4, an FC layer is also acted on the feature maps of soil moisture product, with the result of vector value S_T:

$$S_T = \mathrm{FC}(\mathbf{S}'_4) \; s.t. \; P_T = \mathrm{FC}(\mathbf{P}_T) \tag{3}$$

130   Then the two vectors S_T and P_T of soil moisture product and precipitation product are simultaneously imported into the LSTM module in Fig. 4. The architecture of the LSTM module within the proposed framework is displayed in Fig. 5.
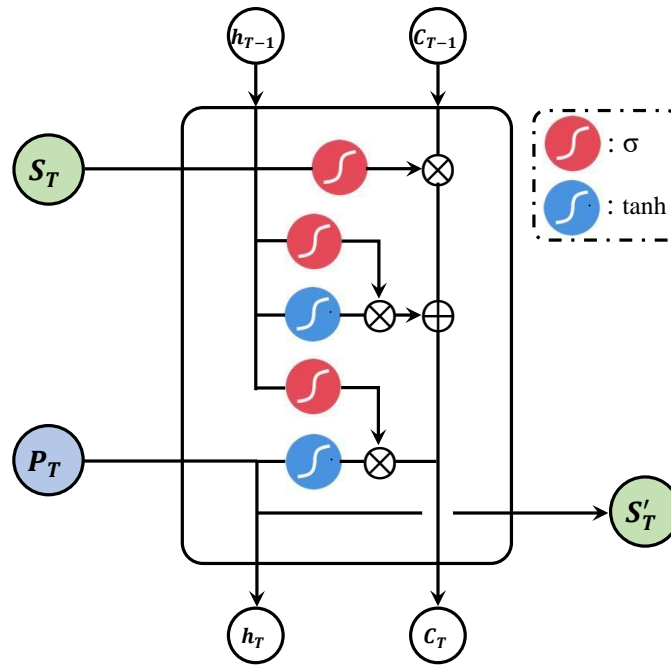
Figure 5. Structure of the LSTM module in the proposed framework.

As depicted in Fig. 5, soil moisture information S_T, corresponding precipitation information P_T, previous long-term memory information C_{T-1}, and previous short-term memory information h_{T-1} are simultaneously imported into the LSTM module. The output values in LSTM are the regenerated soil moisture information S'_T, current long-term memory information C_T, and

135   current short-term memory information h_T. It should be noted that, current long and short-term memory information in date T is the previous long and short-term memory information in next date $T+1$, respectively. For memory information h_0 and C_0, these vectors are initialized with zero elements. LSTM is composed of three gates: Oblivious gate, input gate and output gate to control memory information state (Zhang et al., 2020).

1) Oblivious gate: This gate determines which information needs to be discarded in the short-term memory state. It is carried

140   out by the sigmoid unit σ between the soil moisture information S_T and previous long-term memory information C_{T-1}.

$$f_T = \sigma(W_f \cdot [h_{T-1}, S_T] + b_f) \tag{4}$$

where the sigmoid unit σ is defined below:

$$\sigma(a) = \frac{1}{1 + e^{-a}} \tag{5}$$

In the sigmoid unit σ, zero means fail and one means pass for current information. Through checking the soil moisture information S_T and previous long-term memory information C_{T-1}, it generates a vector between 0 and 1. This variable determines which information is retained or discarded in the short-term memory state.

2) Input gate: This gate determines what new information is added to the long-term memory state. Firstly, we use h_{T-1} and S_T to determine which information needs to be updated through the sigmoid operation in Eq. (6):

$$i_T = \sigma(W_i \cdot [h_{T-1}, S_T] + b_i) \tag{6}$$

Then the new candidate long-term memory information $\tilde{C}_T$ is generated through the tanh unit in Eq. (7):

$$\tilde{C}_T = \tanh(W_C \cdot [h_{T-1}, S_T] + b_C) \tag{7}$$

where the tanh unit is defined as:

$$\tanh(a) = \frac{e^a - e^{-a}}{e^a + e^{-a}} \tag{8}$$

3) Output gate: In this gate, we need to output current long-term memory information C_T from previous C_{T-1} and candidate long-term memory information $\tilde{C}_T$:

$$C_T = f_T \otimes C_{T-1} + i_T \otimes \tilde{C}_T \tag{9}$$

After updating current long-term memory information C_T, the regenerated soil moisture information S'_T is output through previous short-term memory h_{T-1}, soil moisture information S_T, and corresponding precipitation information P_T:

$$S'_T = \sigma(W_{S'}[h_{T-1}, S_T] + b_{S'}) \otimes \tanh(P_T) \tag{10}$$

Besides, we need to output current short-term memory information h_T for the next date $T+1$ as follow:

$$h_T = \tanh(o_T \otimes C_T) \tag{11}$$

Later, the regenerated soil moisture information S'_T is transformed by a FC layer in the right of Fig. 4. Then four partial CNN layers are performed, to generate the final SGD-SM 2.0 product in date T. Through the consecutive time-series strategy, we recursively reconstruct the daily soil moisture products in SGD-SM 2.0.

3.2 Training and optimization

To generate reliable and high-precision SGD-SM 2.0 dataset, how to train and optimize the proposed LSTM-CNN model is extremely crucial in this work. The training stage needs huge numbers of sample labels, to optimize the trainable parameters in the proposed partial CNN and LSTM in Fig. 4 and Fig. 5, respectively. The sample labels adopt patch selecting strategy. We select sequential time-series daily soil moisture patches with $k = 7$ in the reconstructing framework. The spatial size of these seven-day soil moisture patches is all set as 40×40. These time-series seven-day soil moisture patches are all complete,

without gap or data missing regions from the original soil moisture products. Then, we randomly select 30000 mask patches with the size of 40×40. Each soil moisture patch is simulated with missing regions via these mask patches. Through this way, we acquire 30000 training samples from the original 2002-2022 soil moisture products. Each training sample includes four variables: the simulated seven-day soil moisture patches, the complete seven-day soil moisture patches, the corresponding mask patches, and the corresponding precipitation patches. These variables are simultaneously imported into the LSTM-CNN reconstructing model, as shown in Fig. 4.

For the partial CNN in the proposed framework, we set the convolutional filter size as 3×3 in all the partial CNN layers. The last partial CNN layer outputs just one feature map and the other partial CNN layers output 64 feature maps. ReLU is utilized after each partial CNN layer. For the LSTM module in the proposed framework, we set the dimension of long and short-term memory vectors C_T and h_T as 2048.

For the network optimization, we adopt the same strategy with the global-local function (Zhang et al., 2021) in SGD-SM 1.0. The global soil moisture uniformity and local soil moisture heterogeneity are both taken into consideration in the proposed LSTM-CNN reconstructing model. Different from SGD-SM 1.0, we simultaneously fill the gap and missing regions in time-series seven-day soil moisture patches. Detailed definitions of the global-local function are determined as follows:

$$\xi(\mathbf{W}, b, W_{f,i,C,S'}, b_{f,i,C,S'}) = \sum_{T=1}^{k} \left(\left\| (1 - \mathbf{M}_T) \otimes (\mathbf{S}_T^{rec} - \mathbf{S}_T^{ori}) \right\|_2^2 + \left\| (\mathbf{M}_L \otimes (\mathbf{S}_T^{rec} - \mathbf{S}_T^{ori}) \right\|_2^2 \right) \tag{12}$$

where $\mathbf{M}_L$ represents the global land mask (including 6 continents and neglecting all regions of Antarctica and most regions of Greenland). α stands for the balancing parameter to equilibrate the local loss and global loss (Zhang et al., 2020). Empirically, this ratio is fixed as 0.1 in the training and optimization stage.

In terms of the hyper-parameters and operations of the proposed framework, related explanations are listed below. The batch size of the LSTM-CNN reconstructing model is set as 128 (Zhang et al., 2018). The whole epoch number is confirmed determined as 500. The inceptive learning rate is started as 0.005. It gradually decreases through multiplying a damping factor (equal to 0.5) every 100 epochs (Zhang et al., 2019). On software configuration, LSTM-CNN model is carried out on PyTorch 1.8.1 framework. We use Python 3.7 language, PyCharm platform, and Windows 10 environment to generate seamless global daily soil moisture products. On hardware configuration, we employ a NVIDIA Titan X (Pascal) GPU, Inter E5-2609v3 CPU, and 16 GB DDR4 RAM to execute the proposed LSTM-CNN model.

4 Experiments and validations

The released SGD-SM 2.0 products are recorded at **https://doi.org/10.5281/zenodo.6041561** (Zhang et al., 2022). SGD-SM 2.0 starts from 2002.06.23, and ends at 2022.02.05. The initial and reconstructing global daily soil moisture products have been stored with individual NetCDF4 (*.nc) document. Because part of daily soil moisture products is missing at GES DISC, these products are also neglected in the proposed SGD-SM 2.0 dataset (7115 files). In this section, the experimental results of SGD-SM 2.0 dataset are given in section 4.1. Later, we carry out the in-situ validation and time-series validation of SGD-SM 2.0 in section 4.2 and section 4.3, respectively.

4.1 Experimental results

As shown in Fig. 6 and Fig. 7, the SM and SGD-SM 2.0 results are given in 10, 20, and 30 September 2002 and in 10, 20, 205 and 30 June 2020, respectively.

(a) Original SM in 2002.09.10

(b) SGD-SM 2.0 in 2002.09.10

(c) Original SM in 2002.09.20

(d) SGD-SM 2.0 in 2002.09.20

(e) Original SM in 2002.09.30

(f) SGD-SM 2.0 in 2002.09.30
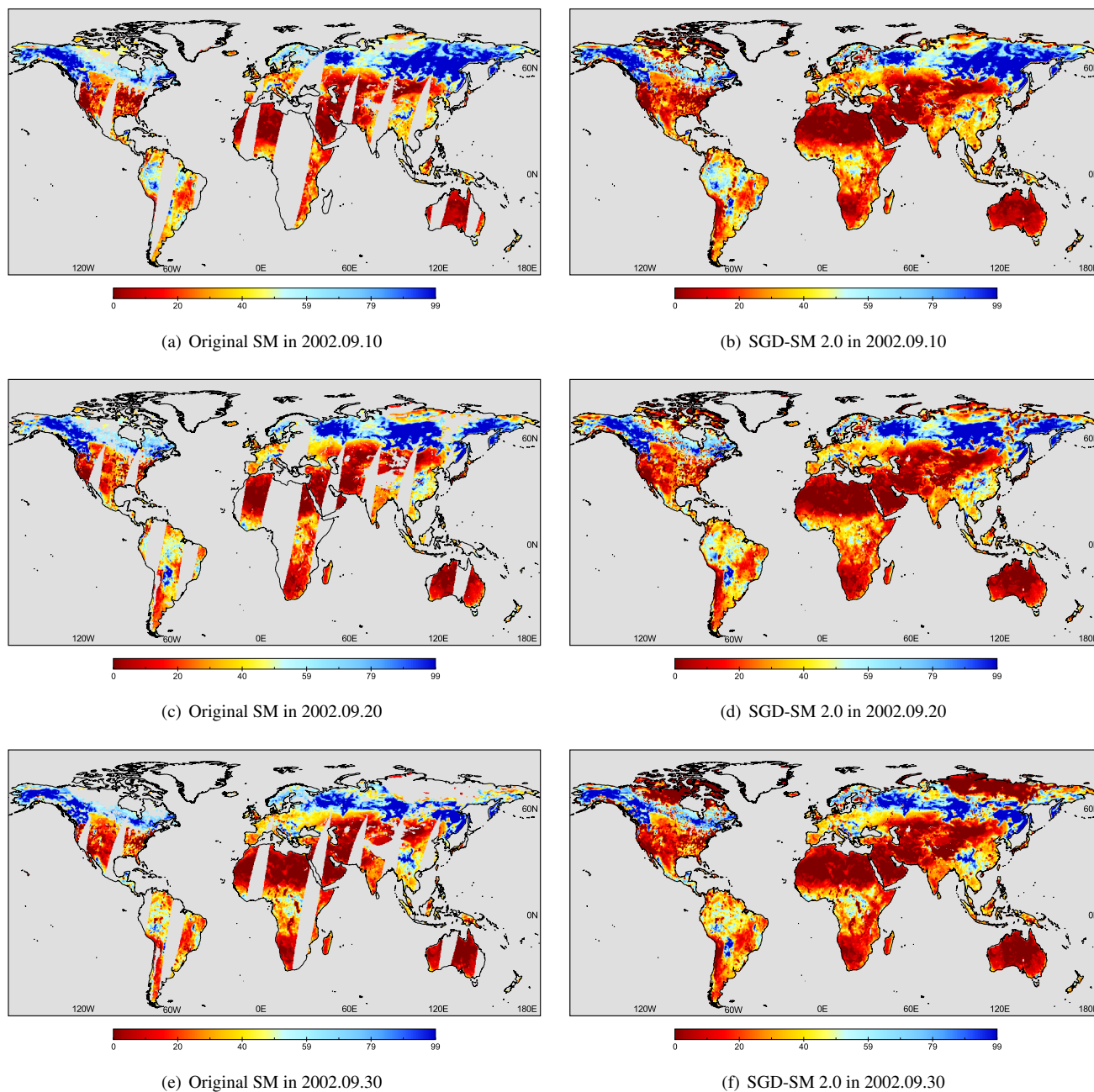
Figure 6. Original SM and proposed SGD-SM 2.0 results in 10, 20, and 30 September 2002.4

For comparison purpose, the left lines are the original global daily products and the right lines are the reconstructed SGD-SM 2.0 products in Fig. 6 and Fig. 7. It should be noted that we neglect all regions in Antarctica and most regions in Greenland, because of the perpetual frozen soil. Clearly, gaps and missing regions are filled through the proposed framework in Sect. 3.

(a) Original SM in 2020.06.10

(b) SGD-SM 2.0 in 2020.06.10

(c) Original SM in 2020.06.20

(d) SGD-SM 2.0 in 2020.06.20

(e) Original SM in 2020.06.30

(f) SGD-SM 2.0 in 2020.06.30
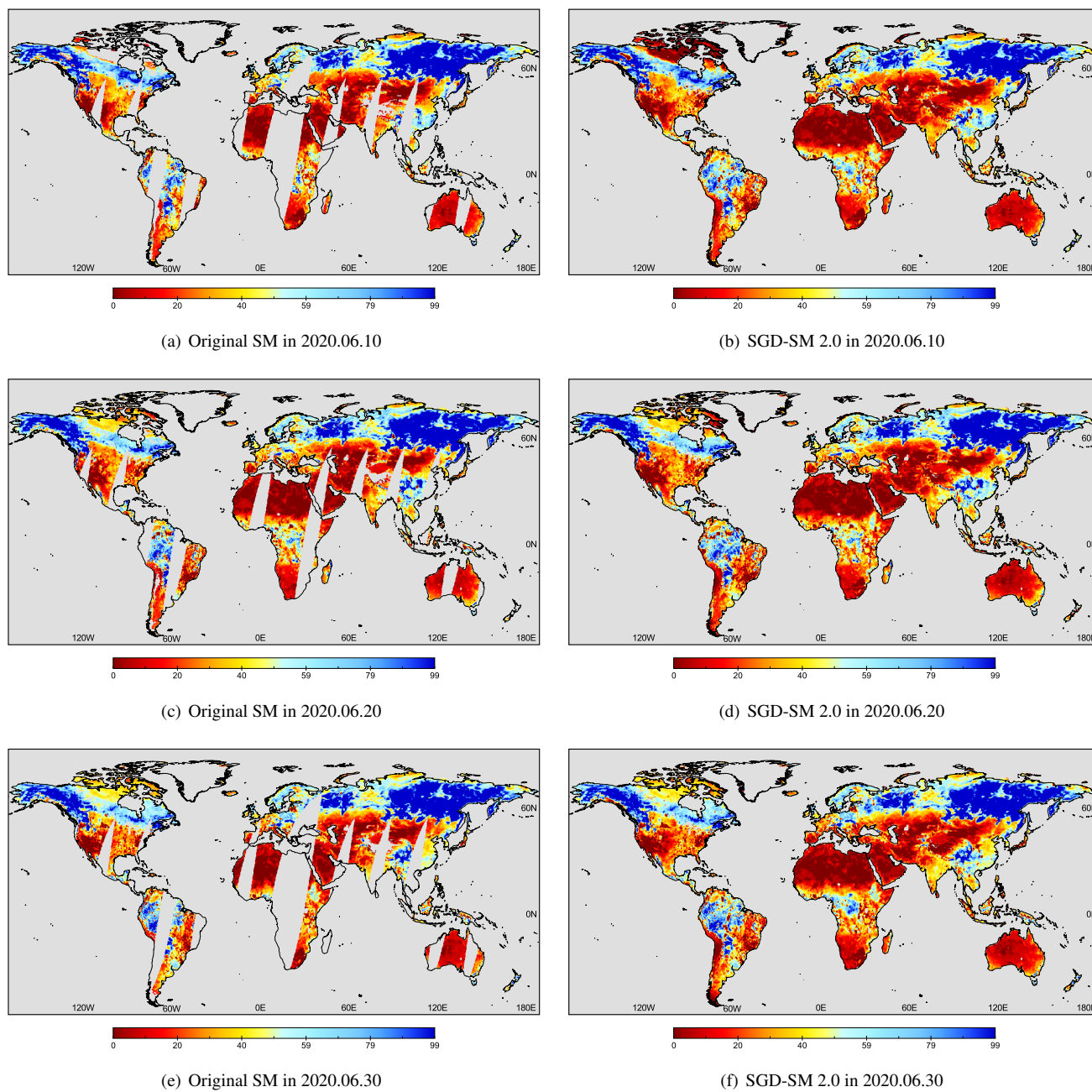
Figure 7. Original SM and proposed SGD-SM 2.0 results in 10, 20, and 30 June 2020.

From the spatial perspective, the proposed SGD-SM 2.0 dataset performs both global soil moisture uniformity and local soil
210 moisture heterogeneity in Fig. 6 and Fig. 7. It ensures the spatial consistency especially for the gap regions with the adjoin soil
moisture regions. Beyond that, the reconstructed regions in SGD-SM 2.0 don't reflect distinct patch or border effect. This also
testifies the powerful ability of partial CNN in the proposed framework, which can effectively exclude the invalid information
in gap or missing soil moisture regions.

From the temporal perspective, the proposed SGD-SM 2.0 dataset utilizes the complementary and sequential time-series
215 soil moisture information. Through drawing into global daily precipitation products, SGD-SM 2.0 can consider the sporadic
extreme weather condition for single day. In addition, by means of LSTM module, the consistent temporal information can be
recovered and preserved in Fig. 6 and Fig. 7.

4.2 In-situ validation
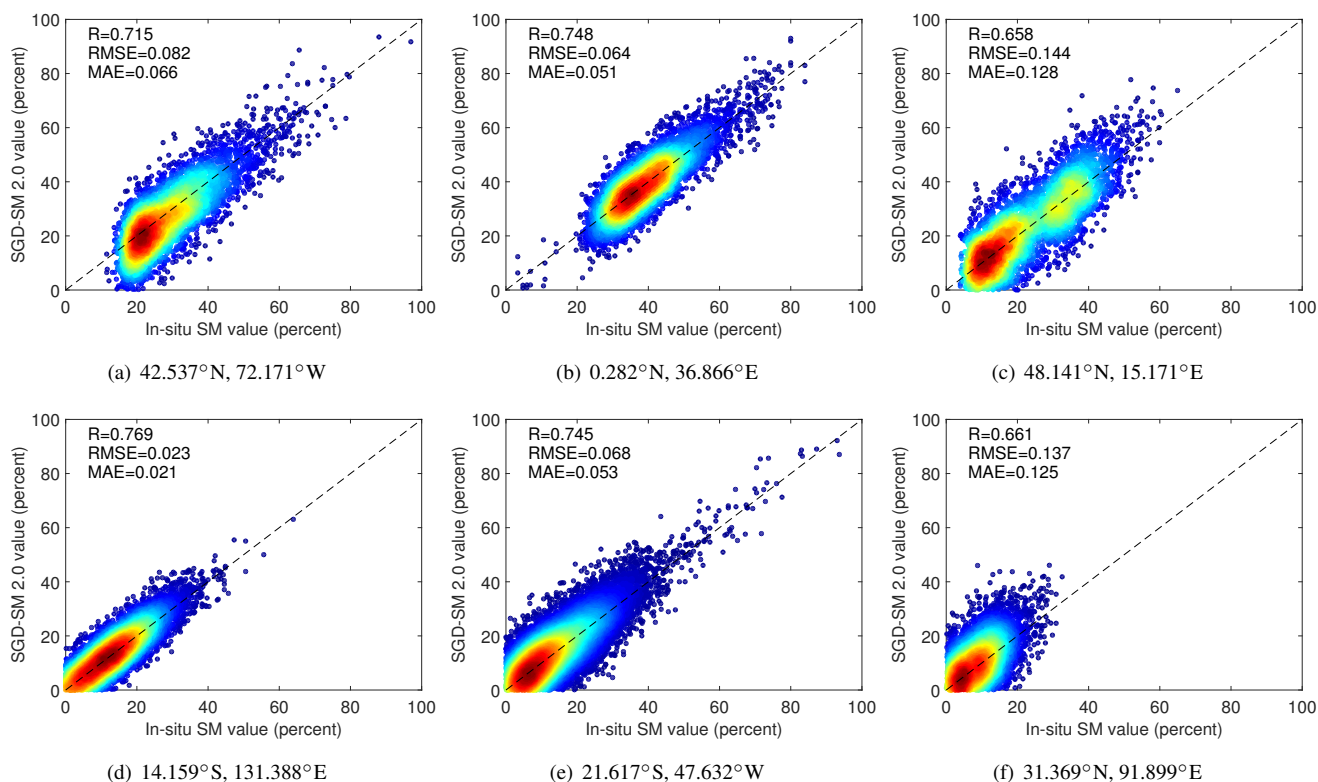
Figure 8. Scatters of six in-situ sites (Horizontal coordinate refers to the in-situ data; Vertical coordinate denotes the reconstructing data).

In-situ validation is the most reliable method to measure the accuracy and availability of the proposed SGD-SM 2.0 dataset
220 (Walker et al., 2004; Draper et al., 2009; Zeng et al., 2015). In this work, we choose 124 in-situ surface (0∼5cm depth) soil
moisture sites from ISMN, as shown in Fig. 2(b). The selected in-site values are limited from 2002 to 2022. We match the

hourly in-site values with the descending products. In consideration of validation reliability, we choose the two neighboring in-site values correspond with the observation time of soil moisture products. Then we average them as the ground-truth data.

As portrayed in Fig. 8, the scatters of six in-situ soil moisture sites (42.537°N, 72.171°W; 0.282°N, 36.866°E; 48.141°N,
225 15.171°E; 14.159°S, 131.388°E; 21.617°S, 47.632°W; 31.369°N, 91.899°E) are displayed to demonstrate the reconstructing accuracy of SGD-SM 2.0. The horizontal coordinate refers to in-situ data. Accordingly, the vertical coordinate denotes reconstructing data in gaps or missing soil moisture regions. The time range is limited from 2002 to 2022. The R indicators of these sites are varied from 0.658 to 0.769 in Fig. 8(a)-(f). The RMSE indicators and MAE indicators of these sites are varied from 0.023 to 0.144 and from 0.021 to 0.128 in Fig. 8(a)-(f), respectively.

230 Through all selected in-situ sites, Table 1 compares the original products with SGD-SM 2.0. The average evaluation indicators (R, RMSE, and MAE) of original soil moisture and SGD-SM 2.0 products are 0.679 (0.672), 0.094 (0.096), and 0.075 (0.078), respectively. Generally, the precision of SGD-SM 2.0 products performs similar with incipient products. The diversities of those indicators are little between the original and reconstructed SGD-SM 2.0 products in Table 1. To a certain extent, in-situ validation testifies the reconstructed accuracy and validity of the SGD-SM 2.0 products.

Table 1. Comparisons between the original and SGD-SM 2.0 products (from 2002 to 2022) through in-situ validation.

Soil moisture products (2002∼2022)	Average evaluation indicators		
	R	RMSE	MAE
Original	0.679	0.094	0.075
SGD-SM 2.0	0.672	0.096	0.078

4.3 Time-series validation
235

Long-term daily soil moisture products usually reflect typical time-series continuity (Liu et al., 2019; Seneviratne et al., 2010). Therefore, we can utilize this characteristic to validate the reliability of SGD-SM 2.0 products. As listed in Fig. 9 and Fig. 10, two time-series daily original/SGD-SM 2.0 results of 2003 to 2018, and 2005 to 2020, are given in the location (10.125°S, 42.625°W) and the location (38.375°N, 117.125°E), respectively. The blue point refers to existing valid value in
240 Fig. 9 and Fig. 10. The red point stands for the SGD-SM 2.0 value in Fig. 9 and Fig. 10, which also represent the invalid gaps or missing soil moisture regions. The vertical coordinate denotes the percent of soil moisture product in original and SGD-SM 2.0 products. The horizontal coordinate denotes the annual date number between 2003 and 2020.

As depicted in Fig. 9(a)-(d) and Fig. 10(a)-(d), a majority of the reconstructed SGD-SM 2.0 values (in invalid gap or missing soil moisture regions) can distinctly embody the time-series continuity. In the two locations of different years, original
245 soil moisture values and corresponding adjacent SGD-SM 2.0 values perform fore-and-aft consistency. If current valid soil moisture values behave high or low, their neighborhood SGD-SM 2.0 values also accord with them in Fig. 9 and Fig. 10. This time-series validation manifests the reliability of proposed framework and validity of our improved SGD-SM 2.0 products.

Generally, the proposed SGD-SM 2.0 products are able to ensure the time-series continuity in daily temporal resolution. This point is greatly important for reconstructing long-term products. Benefiting from the utilizing of temporal information, the
250   proposed LSTM module can extract and transmit time-series features for filling the gap and missing data regions in daily soil moisture products. Therefore, SGD-SM 2.0 can be effectively applied for global hydrology monitoring analyzing at fine temporal scale, rather than the traditional monthly or yearly averaging operation. The former one preserves the original daily temporal resolution, while the latter one sacrifices this daily temporal resolution. This validation exactly demonstrates above significance of the proposed SGD-SM 2.0 dataset.

(a) Time-series daily original/SGD-SM 2.0 results in 2003

(b) Time-series daily original/SGD-SM 2.0 results in 2008

(c) Time-series daily original/SGD-SM 2.0 results in 2013

(d) Time-series daily original/SGD-SM 2.0 results in 2018
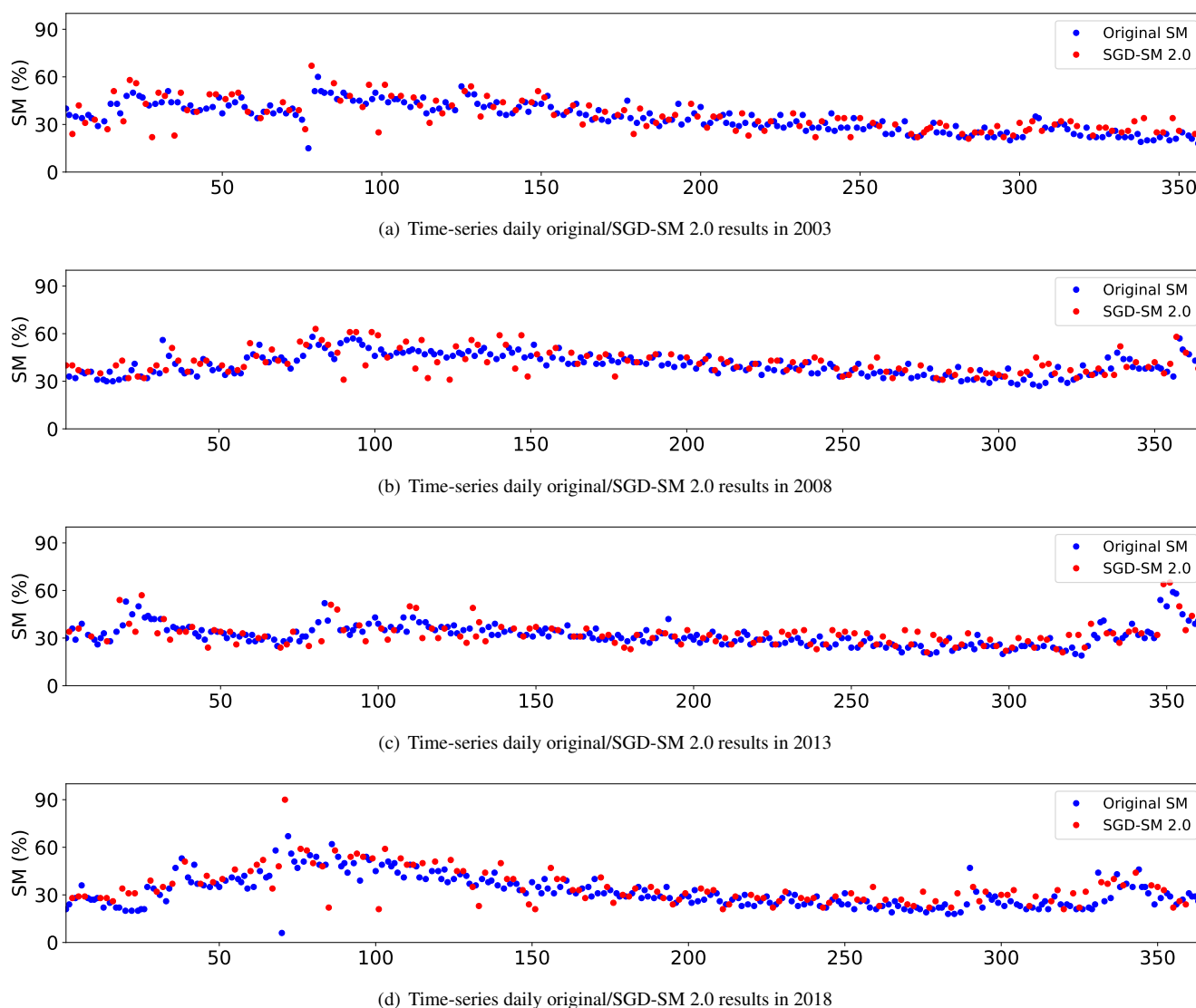
Figure 9. Time-series daily original/SGD-SM 2.0 results of the location (10.125°S, 42.625°W) in 2003, 2008, 2013, and 2018.
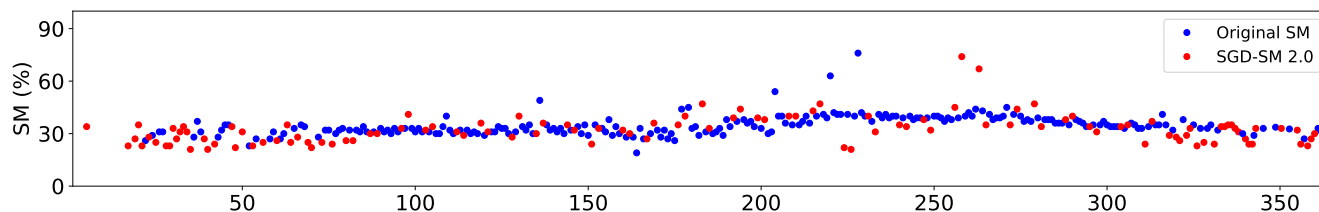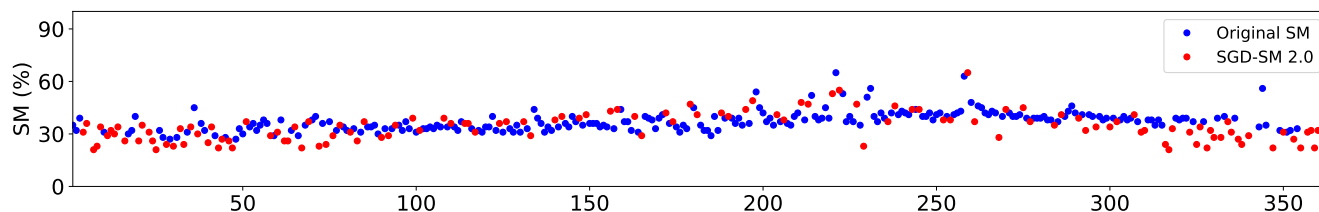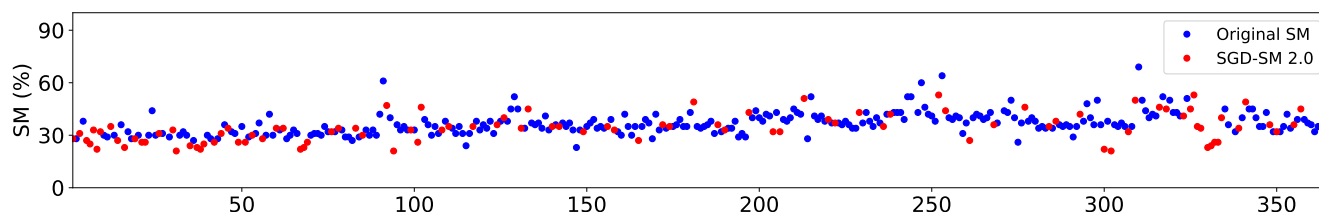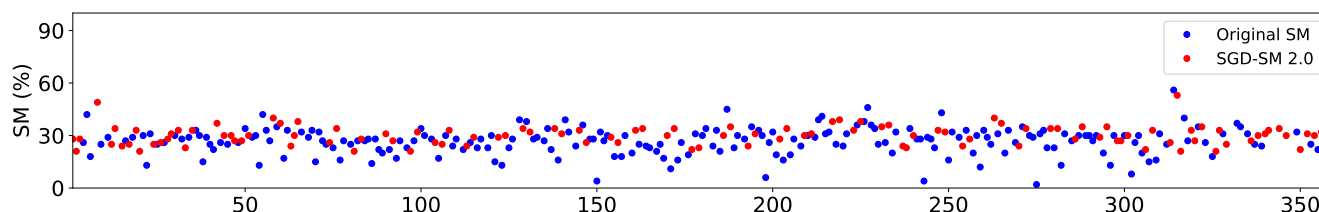
Figure 10. Time-series daily original/SGD-SM 2.0 results of the location (38.375°N, 117.125°E) in 2005, 2010, 2015, and 2020.

255 5 Comparisons with SGD-SM 1.0

In this section, we compare the proposed SGD-SM 2.0 dataset with previous SGD-SM 1.0 dataset, from the perspectives of reconstructing accuracy and time-series consistency. In contrast with SGD-SM 1.0, we assimilate the global daily precipitation products into the reconstructing framework. In addition, the LSTM-CNN model is developed to fill the gap and missing regions in SGD-SM 2.0 global daily soil moisture products. Detailed comparisons between the SGD-SM 1.0 and SGD-SM 2.0

260 are displayed as follows.

5.1 Reconstructing accuracy

For ensuring the same time scope with SGD-SM 1.0, we choose the part of SGD-SM 2.0 from 2013 to 2019. The average evaluation indicators (R, RMSE, and MAE) of SGD-SM 1.0 and SGD-SM 2.0 dataset by selective 124 in-situ sites are contrasted in Table 2.

265   Compared with SGD-SM 1.0 products, SGD-SM 2.0 products outperform on R (0.688), RMSE (0.094), and MAE (0.077). The main reason is that SGD-SM 1.0 ignores the sudden extreme weather condition for one day. If it occurs a sudden precipitation in one day, while there are no abnormalities before and after this day, SGD-SM 1.0 usually behaves with poor performance under this condition. Accordingly, SGD-SM 2.0 introduces the global daily precipitation products into the reconstructing framework. Through assimilating auxiliary precipitation information, SGD-SM 2.0 products can consider the sudden

270 extreme weather condition for single day in global daily soil moisture products. The comparisons validate the effectiveness of this point in Table 2.

Table 2. Comparisons between the SGD-SM 1.0 and SGD-SM 2.0 products (from 2013 to 2019) through selected 124 in-situ sites.

Dataset version	Average evaluation indicators		
	R	RMSE	MAE
SGD-SM 1.0	0.659	0.107	0.083
SGD-SM 2.0	**0.688**	**0.094**	**0.077**

5.2 Time-series consistency

Except the reconstructing accuracy, time-series consistency is also significant for generating seamless daily products (Liu et al., 2020). As portrayed in Fig. 11(a) and (b), we simultaneously depict time-series daily original soil moisture, SGD-SM

275 1.0/2.0, and precipitation results of the location (48.875°N, 140.375°E) in 2013, respectively. The blue point refers to existing valid values in Fig. 11. Red point stands for the SGD-SM 1.0/2.0 value in Fig. 11, which also represent the invalid gap or missing soil moisture regions. The left vertical coordinate denotes the percent of soil moisture product in original and SGD-SM 1.0/2.0 products. The right vertical coordinate refers to the daily precipitation value (unit: mm) by the IMERG level 3 global daily final precipitation products. The horizontal coordinate denotes the date number in 2013.

280   Compared with SGD-SM 1.0, SGD-SM 2.0 outperforms on time-series consistency in Fig. 11(a) and (b). The reconstructed SGD-SM 2.0 points behave more consecutive around their adjacent original soil moistures points than SGD-SM 1.0. While SGD-SM 1.0 exists discrete problem in Fig. 11(a), to some degree. Benefiting from the data assimilation of daily precipitation information, the proposed LSTM module can extract time-series features for filling the gaps and missing regions in daily soil moisture products. Therefore, SGD-SM 2.0 can be effectively utilized for global hydrology monitoring analyzing at fine

285 temporal scale, rather than the traditional monthly or yearly averaging operation.
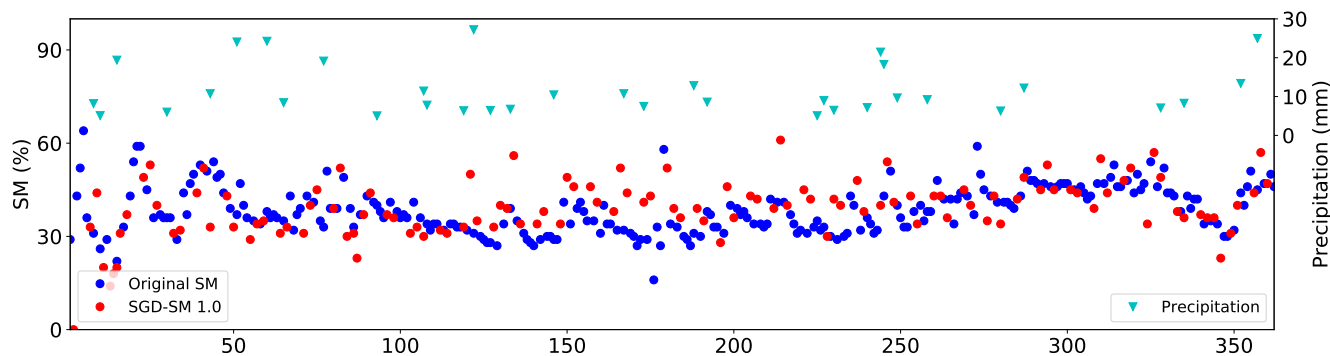
(a) Time-series daily original soil moisture, SGD-SM 1.0, and precipitation results in 2013
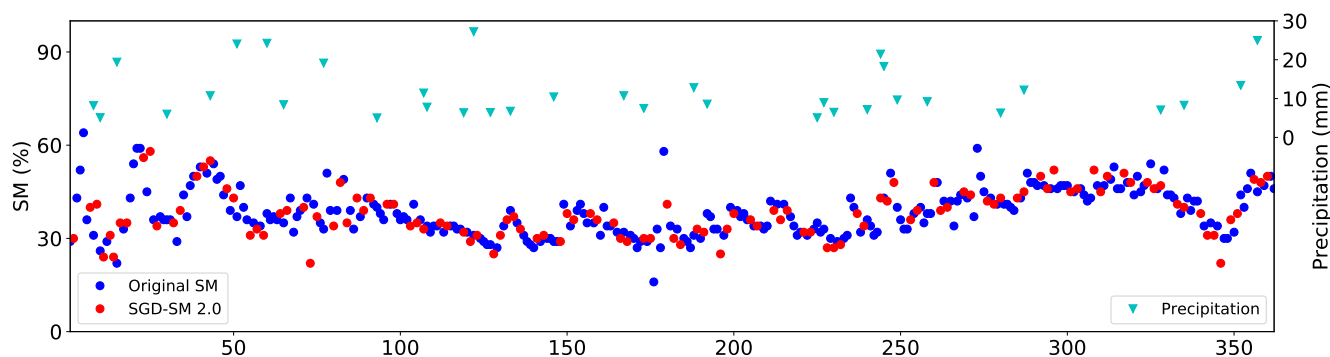
(b) Time-series daily original soil moisture, SGD-SM 2.0, and precipitation results in 2013

Figure 11. Time-series daily original soil moisture, SGD-SM 1.0/2.0, and precipitation results at location (48.875°N, 140.375°E) in 2013.

6 Conclusions

In this paper, we generate an improved seamless global daily soil moisture (SGD-SM 2.0) dataset from 2002 to 2022. Compared with previous SGD-SM 1.0, the temporal range of SGD-SM 2.0 is extended to twenty years from 2002 to 2022. SGD-SM 2.0 assimilates the global daily precipitation products with global daily soil moisture products. In addition, SGD-SM 2.0 develops an integrated LSTM-CNN model to fill the gaps and missing regions. In-situ validation and time-series validation testify the reconstructing accuracy and availability of SGD-SM 2.0 products (R: 0.672, RMSE: 0.096, MAE: 0.078). In contrast with SGD-SM 1.0, the time-series curves of the improved SGD-SM 2.0 products are consistency with the original daily time-series soil moisture values.

In our future work, we will assimilate multi-source data such as global land cover products and land surface temperature into the reconstructed framework. More spatio-temporal model will be exploited to generate the prospective products.

Data availability. The proposed SGD-SM 2.0 dataset could be acquired at **https://doi.org/10.5281/zenodo.6041561** (Zhang et al., 2022).

Author contributions. Q. Z presented the algorithm and carried out the experimental results. QQ. Y, TY. J, and MP. S polished the entire manuscript. FJ. S downloaded soil moisture products and precipitation products in this work. All authors checked and gave related comments for this work.

300 *Competing interests.* The authors declare that they have no conflict of interest.

Acknowledgements. This work was supported in part by the National Natural Science Foundation of China under Grant 41922008, 61971319 and 41701400. We appreciatively acknowledge GES DISC and ISMN, for them releasing related products and in-situ sites.

References

Al Bitar, A., Mialon, A., Kerr, Y. H., Cabot, F., Richaume, P., Jacquette, E., Quesney, A., Mahmoodi, A., Tarot, S., Parrens, M., Al-Yaari, A., Pellarin, T., Rodriguez-Fernandez, N., and Wigneron, J.-P.: The global SMOS Level 3 daily soil moisture and brightness temperature maps, Earth Syst. Sci. Data, 9, 293–315, https://doi.org/10.5194/essd-9-293-2017, 2017.

Berg, P., Almén, F., and Bozhinova, D.: HydroGFD3.0 (Hydrological Global Forcing Data): a 25 km global precipitation and temperature data set updated in near-real time, Earth Syst. Sci. Data, 13, 1531–1545, https://doi.org/10.5194/essd-13-1531-2021, 2021.

Brocca, L., Ciabatta, L., Massari, C., Moramarco, T., Hahn, S., Hasenauer, S., Kidd, R., Dorigo, W., Wagner, W., and Levizzani, V.: Soil as a natural rain gauge: Estimating global rainfall from satellite soil moisture data, J. Geophys. Res. Atmos., 119, 5128– 5141, https://doi.org/10.1002/2014JD021489, 2014.

Brocca, L., Filippucci, P., Hahn, S., Ciabatta, L., Massari, C., Camici, S., Schüller, L., Bojkov, B., and Wagner, W.: SM2RAIN–ASCAT (2007–2018): Global daily satellite rainfall data from ASCAT soil moisture observations, Earth Syst. Sci. Data, 11, 1583–1601, https://doi.org/10.5194/essd-11-1583-2019, 2019.

Brocca, L., Tarpanelli, A., Filippucci, P., Dorigo, W., Zaussinger, F., Gruber, A., Fernández-Prieto, D.: How much water is used for irrigation? A new approach exploiting coarse resolution satellite soil moisture products. Int. J. Applied Earth Obs. Geoinf., 73C, 752–766, https://doi.org/10.1016/j.jag.2018.08.023, 2018.

Brocca, L., Zucco, G., Mittelbach, H., Moramarco, T., Seneviratne, S. I.: Absolute versus temporal anomaly and percent of saturation soil moisture spatial variability for six networks worldwide. Water Resources Research, 50, 5560–5576, http://dx.doi.org/10.1002/2014WR015684, 2014.

Chen, Y., Feng, X., and Fu, B.: An improved global remote-sensing-based surface soil moisture (RSSSM) dataset covering 2003–2018, Earth Syst. Sci. Data, 13, 1–31, https://doi.org/10.5194/essd-13-1-2021, 2021.

Dorigo, W., de Jeu, R., Chung, D., Parinussa, R., Liu, Y., Wagner, W., and Fernández-Prieto, D.: Evaluating global trends (1988–2010) in harmonized multi-satellite surface soil moisture, Geophys. Res. Lett., 39, https://doi.org/10.1029/2012GL052988, 2012.

Dorigo, W. A., Wagner, W., Hohensinn, R., Hahn, S., Paulik, C., Xaver, A., Gruber, A., Drusch, M., Mecklenburg, S., van Oevelen, P., Robock, A., and Jackson, T.: The International Soil Moisture Network: a data hosting facility for global in situ soil moisture measurements, Hydrol. Earth Syst. Sci., 15, 1675–1698, https://doi.org/10.5194/hess-15-1675-2011, 2011.

Dorigo, W. A., Xaver, A., Vreugdenhil, M., Gruber, A., Hegyiová, A., Sanchis-Dufau, A. D., Zamojski, D., Cordes, C., Wagner, W., and Drusch, M.: Global automated quality control of in situ soil moisture data from the international soil moisture network, Vadose Zone J., 12, 1–21, https://doi.org/10.2136/vzj2012.0097, 2013.

Draper, C., Walker, J., Steinle, P., De Jeu, R., Holmes, T. R: An evaluation of AMSR–E derived soil moisture over Australia. Remote Sensing of Environment, 113, 703–710, https://doi.org/10.1016/j.rse.2008.11.011, 2009.

Enenkel, M., Reimer, C., Dorigo, W., Wagner, W., Pfeil, I., Parinussa, R., and De Jeu, R.: Combining satellite observations to develop a global soil moisture product for near-real-time applications, Hydrol. Earth Syst. Sci., 20, 4191–4208, https://doi.org/10.5194/hess-20-4191-2016, 2016.

Fan, Y., and van den Dool, H.: Climate prediction center global monthly soil moisture data set at 0.5° resolution for 1948 to present, J. Geophys. Res., 109, D10102, https://doi.org/10.1029/2003JD004345, 2004.

Guevara, M., Taufer, M., and Vargas, R.: Gap-free global annual soil moisture: 15 km grids for 1991–2018, Earth Syst. Sci. Data, 13, 1711–1735, https://doi.org/10.5194/essd-13-1711-2021, 2021.

340   Liu, X., Pei, F., Wen, Y., Li, X., Wang, S., Wu, C., and Liu, Z.: Global urban expansion offsets climate-driven increases in terrestrial net primary productivity, Nat. Commun., 10, 5558, https://doi.org/10.1038/s41467-019-13462-1, 2019.

Liu, X., Huang, Y., Xu, X., Li, X., Li, X., Ciais, P., and Zeng, Z.: High-spatiotemporal-resolution mapping of global urban change from 1985 to 2015, Nat. Sustain., 3, 564–570, https://doi.org/10.1038/s41893-020-0521-x, 2020.

Long, D., Bai, L., and Yan, L.: Generation of spatially complete and daily continuous surface soil moisture of high spatial resolution, Remote
345   Sens. Environ., 233, 111364, https://doi.org/10.1016/j.rse.2019.111364, 2019.

Long, D., Shen, Y., and Sun, A.: Drought and flood monitoring for a large karst plateau in Southwest China using extended GRACE data, Remote Sens. Environ., 155, 145–160, https://doi.org/10.1016/j.rse.2014.08.006, 2014.

Long, D., Yang W.T., Scanlon, B.R., Zhao, J.S., Liu, D.G., Burek, P., Pan, Y., You, L. Z., Wada, Y.: South-to-North water diversion stabilizing Beijing's groundwater levels. Nat. Comm., 11, 1863–1880, https://doi.org/10.1038/s41467-020-17428-6, 2020.

350   Massari, C., Brocca, L., Pellarin, T., Abramowitz, G., Filippucci, P., Ciabatta, L., Maggioni, V., Kerr, Y., and Fernandez Prieto, D.: A daily 25 km short-latency rainfall product for data-scarce regions based on the integration of the Global Precipitation Measurement mission rainfall and multiple-satellite soil moisture products, Hydrol. Earth Syst. Sci., 24, 2687–2710, https://doi.org/10.5194/hess-24-2687-2020, 2020.

McColl, K. A., Alemohammad, S. H., and Akbar, R.: The global distribution and dynamics of surface soil moisture, Nat. Geosci., 10, 100–104, https://doi.org/10.1038/NGEO2868, 2017.

355   Meng, X., Mao, K., Meng, F., Shi, J., Zeng, J., Shen, X., Cui, Y., Jiang, L., and Guo, Z.: A fine-resolution soil moisture dataset for China in 2002–2018, Earth Syst. Sci. Data, 13, 3239–3261, https://doi.org/10.5194/essd-13-3239-2021, 2021.

Nepal, S., Pradhananga, S., Shrestha, N. K., Kralisch, S., Shrestha, J. P., and Fink, M.: Space–time variability in soil moisture droughts in the Himalayan region, Hydrol. Earth Syst. Sci., 25, 1761–1783, https://doi.org/10.5194/hess-25-1761-2021, 2021.

Njoku, E., Jackson, T., Lakshmi, V., Chan, T., Nghiem, S.: Soil moisture retrieval from AMSR-E, IEEE T. Geosci. Remote Sens., 41,
360   215–229, https://doi.org/10.1109/TGRS.2002.808243, 2003.

Pellarin, T., Tran, T., Cohard, J.-M., Galle, S., Laurent, J.-P., de Rosnay, P., and Vischel, T.: Soil moisture mapping over West Africa with a 30-min temporal resolution using AMSR-E observations and a satellite-based rainfall product, Hydrol. Earth Syst. Sci., 13, 1887–1896, https://doi.org/10.5194/hess-13-1887-2009, 2009.

Rebel, K. T., de Jeu, R. A. M., Ciais, P., Viovy, N., Piao, S. L., Kiely, G., and Dolman, A. J.: A global analysis of soil moisture derived from
365   satellite observations and a land surface model, Hydrol. Earth Syst. Sci., 16, 833–847, https://doi.org/10.5194/hess-16-833-2012, 2012.

Schaffitel, A., Schuetz, T., and Weiler, M.: A distributed soil moisture, temperature and infiltrometer dataset for permeable pavements and green spaces, Earth Syst. Sci. Data, 12, 501–517, https://doi.org/10.5194/essd-12-501-2020, 2020.

Seneviratne, S., Corti, T., Davin, E., Hirschi, M., Jaeger, E., Lehner, I., Teuling, A.: Investigating soil moisture–climate interactions in a changing climate: A review, Earth-Sci. Rev., 99, 125-161, https://doi.org/10.1016/j.earscirev.2010.02.004, 2010.

370   Shi, J., Chen, K. S., Li, Q., Jackson, T. J., O'Neill, P. E. and Tsang, L.: A parameterized surface reflectivity model and estimation of bare-surface soil moisture with L-band radiometer, IEEE T. Geosci. Remote Sens., 40, 2674–2686, https://doi.org/10.1109/TGRS.2002.807003, 2002.

Shi, J., Jiang, L., Zhang, L., Chen, K. S., Wigneron, J. P., Chanzy, A., and Jackson, T. J.: Physically based estimation of bare-surface soil moisture with the passive radiometers, IEEE T. Geosci. Remote Sens., 44, 3145–3153, https://doi.org/10.1109/TGRS.2006.876706, 2006.

375   Shi, J., Jackson, T., Tao, J., Du, J., Bindlish, R., Lu, L., and Chen, K. S.: Microwave vegetation indices for short vegetation covers from satellite passive microwave sensor AMSR-E, Remote Sens. Environ., 112, 4285–4300, https://doi.org/10.1016/j.rse.2008.07.015, 2008.

Škrk, N., Serrano-Notivoli, R., Čufar, K., Merela, M., Črepinšek, Z., Kajfež Bogataj, L., and de Luis, M.: SLOCLIM: a high-resolution daily gridded precipitation and temperature dataset for Slovenia, Earth Syst. Sci. Data, 13, 3577–3592, https://doi.org/10.5194/essd-13-3577-2021, 2021.

380 Sun, L. and Fu, Y.: A new merged dataset for analyzing clouds, precipitation and atmospheric parameters based on ERA5 reanalysis data and the measurements of the Tropical Rainfall Measuring Mission (TRMM) precipitation radar and visible and infrared scanner, Earth Syst. Sci. Data, 13, 2293–2306, https://doi.org/10.5194/essd-13-2293-2021, 2021.

Walker, J., Willgoose, G., Kalma, J.: In situ measurement of soil moisture: a comparison of techniques, J. Hydr., 293, 85–99, https://doi.org/10.1016/j.jhydrol.2004.01.008, 2004.

385 Wang, M., Wigneron, J. P., Sun, R., Fan, L., Frappart, F., Tao, S., Ciais, P.: A consistent record of vegetation optical depth retrieved from the AMSR-E and AMSR2 X-band observations. Int. J. Applied Earth Obs. Geoinf., 105, 102609, https://doi.org/10.1016/j.jag.2021.102609, 2021.

Wang, Y., Mao, J., Jin, M., Hoffman, F. M., Shi, X., Wullschleger, S. D., and Dai, Y.: Development of observation-based global multilayer soil moisture products for 1970 to 2016, Earth Syst. Sci. Data, 13, 4385–4405, https://doi.org/10.5194/essd-13-4385-2021, 2021.

390 Wigneron, J. P., Olioso, A., Calvet, J. C., and Bertuzzi, P.: Estimating root zone soil moisture from surface soil moisture data and soil-vegetation-atmosphere transfer modeling, Water Resour. Res., 35, 3735–3745, https://doi.org/10.1029/1999WR900258, 1999.

Wigneron, J. P., Calvet, J. C., Pellarin, T., Van de Griend, A. A., Berger, M., and Ferrazzoli, P.: Retrieving near-surface soil moisture from microwave radiometric observations: current status and future plans, Remote Sens. Environ., 85, 489–506, https://doi.org/10.1016/S0034-4257(03)00051-8, 2013.

395 Yuan, Q., Zhang, Q., Li, J., Shen, H., and Zhang, L.: Hyperspectral image denoising employing a spatial–spectral deep residual convolutional neural network, IEEE T. Geosci. Remote Sens., 57, 1205–1218, https://doi.org/10.1109/TGRS.2018.2865197, 2019.

Zeng, J., Li, Z., Chen, Q., Bi, H. Y., Qiu, J. X., and Zou, P. F.: Evaluation of remotely sensed and reanalysis soil moisture products over the Tibetan Plateau using in-situ observations, Remote Sens. Environ., 163, 91–110, https://doi.org/10.1016/j.rse.2015.03.008, 2015.

Zeng, J., Li, Z., Chen, Q., and Bi, H.: Method for soil moisture and surface temperature estimation in the Tibetan Plateau using spaceborne
400 radiometer observations, IEEE Geosci. Remote Sens. Lett., 12, 97–101, https://doi.org/10.1109/LGRS.2014.2326890, 2015.

Zeng, J., Chen, K., Cui, C., and Bai, X.: A physically based soil moisture index from passive microwave brightness temperatures for soil moisture variation monitoring, IEEE T. Geosci. Remote Sens., 58, 2782–2795, https://doi.org/10.1109/TGRS.2019.2955542, 2020.

Zhang, P., Zheng, D., van der Velde, R., Wen, J., Zeng, Y., Wang, X., Wang, Z., Chen, J., and Su, Z.: Status of the Tibetan Plateau observatory (Tibet-Obs) and a 10-year (2009–2019) surface soil moisture dataset, Earth Syst. Sci. Data, 13, 3075–3102, https://doi.org/10.5194/essd-
405 13-3075-2021, 2021.

Zhang, Q., Yuan, Q., Zeng, C., Li, X., and Wei, Y.: Missing data reconstruction in remote sensing image with a unified spatial-temporal-spectral deep convolutional neural network, IEEE T. Geosci. Remote Sens., 56, 4274–4288, https://doi.org/10.1109/TGRS.2018.2810208, 2018.

Zhang, Q., Yuan, Q., Li, J., Li, Z., Shen, H., and Zhang, L.: Thick cloud and cloud shadow removal in multitemporal imagery using progres-
410 sively spatio-temporal patch group deep learning, ISPRS J. Photogramm., 162, 148–160, https://doi.org/10.1016/j.isprsjprs.2020.02.008, 2020.

Zhang, Q., Yuan, Q., Li, J., Wang, Y., Sun, F., and Zhang, L.: Generating seamless global daily AMSR2 soil moisture (SGD-SM) long-term products for the years 2013-2019, Earth Syst. Sci. Data, 13, 1385–1401, https://doi.org/10.5194/essd-13-1385-2021, 2021.

Zhang, Q., Yuan, Q., Li, Z., Sun, F., and Zhang, L.: Combined deep prior with low-rank tensor SVD for thick cloud removal in multitemporal
415   images, ISPRS J. Photogramm., 176, 125–137, https://doi.org/10.1016/j.isprsjprs.2020.04.010, 2021.

Zhang, Q., Yuan, Q., and Jin, T.: SGD-SM 2.0, Zenodo, https://doi.org/10.5281/zenodo.6041561, 2022.

Zhan, W., Pan, M., Wanders, N., and Wood, E. F.: Correction of real-time satellite precipitation with satellite soil moisture observations,
       Hydrol. Earth Syst. Sci., 19, 4275–4291, https://doi.org/10.5194/hess-19-4275-2015, 2015.

Zhao, T., Shi, J., Entekhabi, D., Jackson, T. J., Hu, L., Peng, Z., Yao, P., Li, S., Kang, C. S.: Retrievals of soil moisture and vegetation optical
420   depth using a multi-channel collaborative algorithm, Remote Sens. Environ., 257, 112321, https://doi.org/10.1016/j.rse.2021.112321,
       2021.